

Accepted to AJ, Jan 2003 issue

Variability-Selected Quasars in MACHO Project Magellanic Cloud Fields

M. Geha¹, C. Alcock^{2,3,4}, R.A. Allsman⁵, D.R. Alves⁶, T.S. Axelrod⁷, A.C. Becker⁸,
D.P. Bennett^{3,9}, K.H. Cook^{3,4}, A.J. Drake^{3,10}, K.C. Freeman¹¹, K. Griest¹², S.C. Keller³
M.J. Lehner², S.L. Marshall³, D. Minniti¹⁰, C.A. Nelson^{3,13}, B.A. Peterson¹¹, P. Popowski¹⁴,
M.R. Pratt¹⁵, P.J. Quinn¹⁶, C.W. Stubbs^{4,15}, W. Sutherland¹⁷, A.B. Tomaney¹⁵, T. Vandehei¹²,
D.L. Welch¹⁸

(The MACHO Collaboration)

ABSTRACT

We present 47 spectroscopically-confirmed quasars discovered behind the Magellanic Clouds identified via photometric variability in the MACHO database. Thirty-eight

¹UCO/Lick Observatory, University of California, Santa Cruz, 1156 High Street, Santa Cruz, CA 95064
Email: mgeha@ucolick.org

²Department of Physics and Astronomy, University of Pennsylvania, Philadelphia, PA, 19104-6396
Email: alcock, mlehner@hep.upenn.edu

³Lawrence Livermore National Laboratory, Livermore, CA 94550
Email: kcook, adrake, skeller, cnelson, stuart@igpp.ucllnl.org

⁴Center for Particle Astrophysics, University of California, Berkeley, CA 94720

⁵NOAO, 950 North Cherry Ave., Tucson, AZ 85719
Email: robyn@noao.edu

⁶Columbia Astrophysics Laboratory, MailCode 5247, 550 W. 120th St., NY, NY, 10027
Email: alves@astro.columbia.edu

⁷Steward Observatory, University of Arizona, Tucson, AZ 85721
Email: taxelrod@as.arizona.edu

⁸Bell Laboratories, Lucent Technologies, 600 Mountain Avenue, Murray Hill, NJ 07974
Email: acbecker@physics.bell-labs.com

⁹Department of Physics, University of Notre Dame, IN 46556
Email: bennett@bustard.phys.nd.edu

¹⁰Depto. de Astronomia, P. Universidad Catolica, Casilla 306, Santiago 22, Chile
Email: dante@astro.puc.cl

¹¹Research School of Astronomy and Astrophysics, Mount Stromlo Observatory, Cotter Road, Weston, ACT 2611, Australia
Email: kcf, peter@mso.anu.edu.au

¹²Department of Physics, University of California, San Diego, CA 92093
Email: kgriest@ucsd.edu, vandehei@astrophys.ucsd.edu

¹³Department of Physics, University of California, Berkeley, CA 94720

¹⁴Max-Planck-Institute für Astrophysik, Karl-Schwarzschild-Str. 1, 85748 Garching bei München, Germany
E-mail: popowski@mpa-garching.mpg.de

¹⁵Departments of Astronomy and Physics, University of Washington, Seattle, WA 98195
Email: stubbs@astro.washington.edu

¹⁶European Southern Observatory, Karl-Schwarzschild-Str. 2, 85748 Garching bei München, Germany
Email: pjq@eso.org

¹⁷Department of Physics, University of Oxford, Oxford OX1 3RH, U.K.
Email: w.sutherland@physics.ox.ac.uk

¹⁸Department of Physics and Astronomy, McMaster University, Hamilton, Ontario, Canada, L8S 4M1
Email: welch@physics.mcmaster.ca

quasars lie behind the Large Magellanic Cloud and nine behind the Small Magellanic Cloud, more than tripling the number of quasars previously known in this region. The quasars cover the redshift interval $0.2 < z < 2.8$ and apparent mean magnitudes $16.6 \leq \overline{V} \leq 20.1$. We discuss the details of quasar candidate selection based on time variability in the MACHO database and present results of spectroscopic follow-up observations. Our follow-up detection efficiency was 20%; the primary contaminants were emission-line Be stars in Magellanic Clouds. For the 47 quasars discovered behind the Magellanic Clouds plus an additional 12 objects previously identified in this region, we present 7.5-year MACHO V - and R -band lightcurves with average sampling times of 2-10 days.

Subject headings: galaxies: kinematics and dynamics — Magellanic Clouds — quasars: general — surveys

1. Introduction

Techniques to find quasars, largely successful in other regions of the sky, have had limited results towards the Magellanic Clouds (Tinney 1999; Schmidtke et al. 1999; Dobrzycki et al. 2002). Crowding, recent star formation and significant dust extinction cause major quasar surveys to avoid these regions entirely, resulting in very few quasars known over the substantial sky coverage of the Magellanic Clouds. The most successful selection method to date in this region has been at X-ray wavelengths. Although many tens of sources background to the Magellanic Clouds have been identified in the X-rays (Kahabka et al. 1999; Haberl & Pietsch 1999; Sasaki, Haberl & Pietsch 2000), counterparts to these sources at other wavelengths have been stymied by positional uncertainties; targeted X-ray follow-up has allowed optical identification of ~ 20 extragalactic sources in the Magellanic Cloud region (Crampton et al. 1997; Schmidtke et al. 1999). The MACHO lightcurve database (Alcock et al. 1997, 2000) provides an opportunity to search for quasars behind the Magellanic Clouds via an alternative method: optical variability.

Optical variability has been studied by many groups as a means of constraining models of the quasar central engine (Hook et al. 1994; Cristiani et al. 1997; Sirola et al. 1998; Hawkings 2002, and references therein), as well as a method of quasar identification behind globular clusters (Meusinger & Brunzendorf 2002). Although a handful of gravitationally-lensed quasars have well-sampled lightcurves on the timescale of years (Alcalde et al. 2002; Hjorth et al. 2002), most studies have had short time baselines and poor resolution. In one of the largest optical monitoring programs, Giveon et al. (1999) observed a sample of 42 quasars over 7 years with an average sampling interval of 40 days. Long-term optical variability of quasars in this study show no strong evidence for underlying periodic structure. This is in sharp contrast to the majority of stellar sources in the Magellanic Clouds which either do not vary or do so periodically. We have used this difference to separate quasar candidates from the overwhelming stellar background in the Clouds.

A comprehensive search for quasars behind both the Large and Small Magellanic Clouds (LMC

and SMC, respectively) is motivated in part by the lack of a suitable reference frame against which to measure the proper motion of the Clouds. Previous proper motion estimates have suffered from an insufficient number or poorly distributed set of reference objects (Jones, Klemola & Lin 1994; Kroupa & Bastian 1997; Anguita, Loyola & Pedreros 2000). Since the proper motion of the Clouds is expected to be only a few mas/year, a well distributed set of point-like background quasars could significantly improve the accuracy of this measurement, constraining the orbital history of these galaxies. These objects may also prove useful as light beacons for absorption line studies of the interstellar medium in the Magellanic Clouds (Gibson et al. 2000; Prochaska, Ryan-Weber & Staveley-Smith 2002), as has been done for suspected extragalactic X-ray sources in this region (Kahabka et al. 2001; Haberl et al 2001). Finally, this search was also motivated by interest in the quasars themselves, in hope that the dense time sampling of the MACHO lightcurves will provide clues to the physical mechanisms underlying quasar light variation.

We discuss the MACHO database and our optical variability quasar candidate selection methods in § 2. In § 3, we describe spectroscopic follow-up observations and present 47 quasars discovered behind the Magellanic Clouds. In § 4, MACHO lightcurves are presented for these quasars. Finally, in § 5 we summarize our results and discuss future quasar searches in this region. Finding charts, light curves and spectra for the quasars in this paper are available on request from the authors or on a website given at the end of § 5.

2. Quasar Candidate Selection

2.1. The MACHO Database

The MACHO project monitored the Magellanic Clouds for the purpose of detecting microlensing events between 1992 July and 2000 January (Alcock et al. 1997, 2000). The Mount Stromlo Observatory 1.27-meter telescope system provided simultaneous imaging in a red ($\lambda\lambda 5900\text{--}7800\text{\AA}$) and blue ($\lambda\lambda 4370\text{--}5900\text{\AA}$) filter, over a $0.5 \square^\circ$ field of view with a scale of $0.63''$ per pixel. We monitored 82 fields ($35 \square^\circ$) in the LMC, and 6 fields ($2.5 \square^\circ$) in the SMC; the location of these fields is shown in Figures 1 and 2. Average sampling frequencies varied from 2 to 10 days between fields. Exposure times were 300-s and 600-s for the LMC and SMC, respectively. Photometric transformations from MACHO passbands to standard V - and R -band magnitudes proceeded using the calibrations discussed in Alcock et al. (1999). Since the MACHO passbands are non-standard and these photometric transformation were determined for stars and not for emission-line quasars, the $(V - R)$ quasar colors in this paper should be approached with caution. We consider only measurements with photometric errors less than 5%; the average MACHO quasar lightcurve contains 600 good photometric measurements over 7.5 years.

Selection of the quasar candidates, described below, was performed on the first 5.7 years of MACHO data; the final 7.5-year MACHO light curves are presented in the lightcurve analysis of § 4. Due to limited data access at the time of selection in the outer LMC MACHO fields, the variability

search discussed in § 2.2 was spatially restricted to the SMC and 30 MACHO LMC fields. In § 2.3, the full spatial coverage of the MACHO database was searched for variable counterparts to known radio and X-ray sources. The final MACHO Magellanic Cloud database, 37.5sq° over 7.5 years, has recently become readily accessible and variability selection will be run on the outer LMC fields not analysed in this paper.

2.2. Quasar Candidate Variability Selection

At the time of candidate selection, the long-term optical photometric behavior of quasars was not adequately constrained to fully automate quasar selection in the MACHO database. Instead, the selection method was designed to automatically reject known classes of variable stars, with the final step being a selection by eye. The MACHO database contained 9 Active Galactic Nuclei (AGN) listed in Table 1 which had been previously cross-identified with X-ray sources by Schmidtke et al. (1999) and one AGN which was serendipitously discovered by Blanco & Heathcote (1986). Two additional sources in the MACHO database were presented by Dobrzycki et al. (2002) subsequent to candidate selection. Lightcurves for these sources, shown in Figure 3, provided a training set around which the selection method was developed. The final subjective step was to select, by eye, lightcurves similar to these known sources. Since our goal was to identify a robust set of quasars, rather than a complete census of quasars behind the Clouds, we deemed this level of subjectivity to be acceptable.

Variability selection was run on 30 MACHO LMC fields (15sq°) containing 12 million objects and 6 MACHO SMC fields (2.5sq°) containing 2 million objects. Candidate selection began with the Level 1 MACHO database, a data subset containing 140,000 objects flagged as having a significant deviation from a constant brightness lightcurve (Alcock et al. 2000). We required objects to have a minimum of 50 photometric measurements in V - and R -bands. Weighted average magnitudes were calculated from the standard equation:

$$\bar{V} \equiv \sum_{i=1}^N \frac{V_i}{\sigma_{V,i}^2} / \sum_{i=1}^N \frac{1}{\sigma_{V,i}^2}. \quad (1)$$

where N is the total number of individual photometric measurements V_i with associated errors $\sigma_{V,i}$. We considered candidates between $16 \leq \bar{V} \leq 20$ which is one magnitude brighter (fainter) than the MACHO photometric completeness (saturation) limits. Candidates were required to have weighted average colors bluer than $(\overline{V-R}) \leq 1.0$. This color cut eliminated long-period quasi-periodic variable stars, while retaining all of the training set AGNs. An example lightcurve of a long period variable is shown in the top right panel of Figure 4; the majority of these stars are extremely red and otherwise difficult to remove from the final quasar candidate list.

Two statistics were used to quantify the amount of lightcurve variability. First, the intrinsic

variability for each candidate quasar lightcurve was calculated as:

$$\widehat{\sigma}_V \equiv \sqrt{\frac{\sum (V_i - \bar{V})^2}{N - 1} - \frac{\sum \sigma_{V,i}^2}{N}} \quad (2)$$

This quantity is an estimate of the true source variability in the absence of photometric errors. The first term is the total variance measured from the lightcurve data, while the second is an estimate of the variance due to photometric measurement errors alone. We note that the photometric error estimate supplied by the photometry code Sodophot (Alcock et al. 1997) is known to have some bias for bright stars. This bias is on the order of 0.01 magnitudes and should have only a small effect on the current data. Giveon et al. (1999) monitored a sample of 42 quasars monthly for 7 years, measuring intrinsic variabilities between $0.05 \leq \widehat{\sigma}_B \leq 0.32$ in the B -band. We therefore require the intrinsic variability of MACHO candidate quasars to be larger than 0.05 magnitudes ($\widehat{\sigma}_V \geq 0.05$). The second variability statistic calculated for each lightcurve is the variability index (Welch & Stetson 1993). This index is a measure of correlated variability between the MACHO V - and R -bands, defined as:

$$I \equiv \sqrt{\frac{1}{N(N-1)} \sum_{i=1}^N \left(\frac{V_i - \bar{V}}{\sigma_{V,i}} \right) \left(\frac{R_i - \bar{R}}{\sigma_{R,i}} \right)} \quad (3)$$

This quantity approaches zero for uncorrelated variability. Quasar variability is expected to be highly correlated between the MACHO passbands; we require $I \geq 1.5$ for our candidates. This limit was set slightly below the minimum I -value determined from the training set AGN. Due to MACHO noise characteristics the two variability statistics described above are not redundant. Systematic noise terms in the MACHO system which affect a single filter can cause large $\widehat{\sigma}_V$ values, but may be eliminated as this variability is not correlated in the second filter. Conversely, variable observing conditions, such as seeing and sky brightness, can cause correlated variability, but these measurements often have large photometric errors and can be rejected based on our $\widehat{\sigma}_V$ cut.

Periodic variable stars, such as Cepheid and RR Lyrae stars, were removed using the MACHO Variable Star Catalogue. This catalogue contains period information for the majority of variable MACHO objects as determined from a super-smoother algorithm which models folded lightcurves (Cook et al. 1995). We reject as candidate lightcurves for which a period (τ) was found at high significance in both passbands over the range $0.1 \leq \tau \leq 500$ days. This cut did not include aliased frequencies ($\tau = 1/n$ days, $n=1,2,\dots$). An example lightcurve of a typical RR Lyrae star in the MACHO database rejected by our periodicity cut is shown in the top right panel of Figure 4.

In the final quasar candidate selection step, each candidate lightcurve was examined by eye to remove objects with spurious noise characteristics or quasi-periodic components. Roughly 2500 light curves were examined by eye; a total of 360 lightcurves were considered candidate quasars. A fraction of lightcurves rejected by eye were due to noise effects above the thresholds set by our variability cuts. However, the majority of rejected candidates were quasi-periodic lightcurves characteristic of blue variable stars, known to the microlensing community as a 'Bumper' stars

(Cook et al. 1995). An example of such a lightcurve is shown in the bottom left panel of Figure 4. These stars typically have strong Balmer emission lines at the velocity of the Clouds and are associated with the Be star phenomena (Keller et al. 2002). These blue variables often have quasi-repeatable outbursts and can be eliminated from the candidate list. As designed, our quasar selection technique successfully recovered all of the previously known quasar/AGNs in the search region.

2.3. Additional Candidate Selection Methods

We have additionally searched for optically-variable counterparts in the error boxes of suspected extragalactic radio and X-ray sources in several Magellanic Cloud surveys. This allowed us to extend our search to the full spatial coverage of the MACHO database (37.5°), as explained in § 2.1. In the LMC, we have searched the LMC radio catalogues of Marx, Dickey & Mebold (1997) and Filipovic et al. (1998) and the X-ray catalogue of Haberl & Pietsch (1999); in the SMC we have searched the radio catalogue of Filipovic et al. (1997) and the X-ray catalogues of Kahabka et al. (1999) and Sasaki, Haberl & Pietsch (2000). Photometric constraints, described in the previous section, are relaxed in this search: any aperiodic MACHO variable ($\widehat{\sigma}_V > 0$) inside the 1σ spatial error box of a cataloged source (typically $\sim 15''$) is considered a candidate. We identified variable, aperiodic MACHO counterparts in the 1σ error boxes for $\sim 5\%$ of the cataloged objects. In the last column of Tables 2 and 3, we note which quasars were identified by this method.

3. Spectroscopic Confirmation of 47 MACHO Quasars

Follow-up spectroscopic observations for our quasar candidates were obtained with the Anglo-Australian Telescope and 2dF multifiber spectrograph (AAT+2dF) in 1999 October and 2001 January. Additional observations were made with the Australian National University 2.3m and Double Beam Spectrograph (ANU+DBS) over 8 nights between 1999 March and 2000 November. The AAT+2dF is a fiber-fed spectrograph with $\sim 2''$ diameter fibers and 200 fibers available per pointing. These observations were made through the 300B grating covering $\lambda\lambda 3800\text{--}7800\text{\AA}$ with 4.3\AA pixels. The 2dF data were reduced using the standard 2dFdr reduction pipeline software (Bailey, Glazebrook & Bridges 2002). Observations with the ANU+DBS were made through a single, $2''$ wide slit in combination with a low resolution 2.2\AA per pixel blue grating ($\lambda\lambda 3500\text{--}6000\text{\AA}$) and a red 4.0\AA per pixel grating ($\lambda\lambda 6000\text{--}9000\text{\AA}$). These data were reduced with IRAF single long-slit spectra reduction procedures. A total of 259 candidate quasars were observed: spectra for 220 candidates were obtained in six separate AAT+2dF pointings, 39 candidates were observed in single pointing with the 2.3m+DBS. The remaining ~ 100 candidates will be observed in future observing runs.

Spectroscopic follow-up revealed a total of 47 previously unknown quasars behind the Magel-

lanic Clouds: 38 behind the LMC and 9 quasars behind the SMC. The quasars cover the redshift interval $0.2 < z < 2.8$ and range in apparent magnitude between $16.6 \leq \bar{V} \leq 20.1$ mag. For the majority of objects, redshifts were determined from two or more broad lines; rest-frame spectra for all 47 newly discovered quasars are shown in Figure 5. All objects appear unresolved in MACHO images. Absolute magnitudes were computed assuming a consensus cosmology of $\Omega_m = 0.3$, $\Omega_\Lambda = 0.7$ and $H_0 = 75 \text{ km s}^{-1} \text{ Mpc}^{-1}$ and are corrected for reddening. Values for reddening vary in the Magellanic Clouds due to patchy dust distribution, and accurate estimates do not yet exist in the directions of all of our quasars. We instead adopted, for each Cloud, a single reddening value of $E(B - V) = 0.12$ and 0.05 (Dutra et al. 2001) for the LMC and SMC, respectively, and a Galactic extinction law.

The spatial distribution of the discovered MACHO quasars is shown relative to the Magellanic Clouds in Figures 1 and 2. In the LMC, quasars appear concentrated to the South of the LMC bar due to several 2dF spectroscopic pointings in this region. Given that ~ 100 quasar candidates have not yet been spectroscopically followed up in this region, and subjectivity in the candidate selection process, our quasar sample is unlikely to be complete. In Tables 2 and 3 we list for each source a MACHO ID number, equatorial coordinates $\alpha(\text{J2000})$ and $\delta(\text{J2000})$, weighted average apparent \bar{V} magnitude and $(\bar{V} - \bar{R})$ color, the redshift, z , the mean absolute magnitude, M_V , and the number of V -band photometric measurements, n_V , available in the MACHO database. We also note if the object was selected as a candidate based on optical variability inside the error box of a suspected extragalactic radio and X-ray source. Histograms of the quasars, distributed as a function of redshift, apparent and absolute magnitude, are shown in Figure 8.

3.1. Candidate List Contamination: Be/Ae Stars

The primary contamination during spectroscopic follow-up of our quasar candidates were emission-line main sequence stars (Be/Ae stars) in the Magellanic Clouds. These stars display strong Balmer emission/absorption lines at the velocity of the Clouds and are known to be photometrically variable (Hubert & Floquet 1998). Of the 258 quasar candidates observed, 188 were emission-line Be/Ae stars. The brightest ($V \leq 16.5$), more well studied, emission-line stars have a strong periodic component to their lightcurves (‘Bumpers’; Cook et al. 1995) and were already removed from the quasar candidate list. However, fainter Be/Ae stars appear to be quasi- to aperiodic variables and were thus included as quasar candidates. An example Bumper light curve is compared to a fainter Be/Ae star in the bottom panels of Figure 4. These objects have very similar spectra, despite significantly different lightcurve behavior. A preliminary analysis of this type of blue variable star is presented in Keller et al. (2002).

4. MACHO Quasar Lightcurves

V -band lightcurves for all quasars listed in Tables 1, 2 and 3 are presented in Figures 3, 6, and 7. The lightcurves have on average 600 photometric measurements in both V - and R -band, spanning 7.5 years. The zero point of the time axis of these plots corresponds to JD 2448623.5, or UT 1992 January 2.0. We have searched for close quasar pair candidates in a $15''$ radius around each source, but find no aperiodic lightcurves at these distances. We note that, unlike the previously discovered sources listed in Table 1 which are predominately AGN, the majority of MACHO sources would be classified as quasars based on the usual absolute luminosity criteria of $M_B = -23$ (strict classification is prohibited by the fact that we determine M_V rather than M_B magnitudes).

Similar to the results of Giveon et al. (1999), we find that the majority of quasars become bluer in $(V - R)$ as they brighten. To quantify this, we calculate the Spearman’s rank correlation probability (P_r) between magnitude and color measurements for each source. The correlation is in the same sense for all quasars (bluer $V - R$ colors at brighter V magnitudes), and is highly significant at a 4.5σ level or greater ($P_r < 3 \times 10^{-5}$) for 95% of the quasar lightcurves. In contrast, the majority (63%) of contaminating Be/Ae stars in our spectroscopic sample became redder as they brightened at similar significance levels. This distinction will be used to improve future quasar selection criteria.

In Figure 9, the V -band intrinsic variability, as defined in Eqn. 2, is plotted as a function of quasar absolute luminosity and redshift. For the more homogeneous subset of quasars discovered via our variability-only method (Fig. 9, solid points), we find according to the Spearman’s rank test, a very weak correlation at the 2.2σ level between variability and absolute luminosity ($\widehat{\sigma}_V - M_V$) in the sense that intrinsically luminous quasars tend to be less variable. For the full set of objects shown in Figure 9, the same correlation between $\widehat{\sigma}_V - M_V$ was more significant at the 3.3σ level. No correlation was found between the intrinsic source variability and redshift ($\widehat{\sigma}_V - z$) for our quasar subset. For the full set, a weak negative correlation between variability and redshift is detected at the 2.5σ level. Several groups have claimed a similar correlation between variability and absolute luminosity (Hook et al. 1994; Cristiani et al. 1997; Giveon et al. 1999), however, both positive and negative correlations have been claimed between variability and redshift. These results are difficult to interpret due to strong correlations between redshift and absolute luminosity, as well as varying definitions of variability. The quasar light curves presented in this paper have sufficient time resolution to allow power spectrum and other detailed lightcurve analyses. It is hoped that such work will be easier to interpret and have interesting implications for the physical mechanisms driving the AGN/quasar variability.

5. Discussion and Summary

We present 47 quasars discovered behind the Magellanic Clouds: 38 behind the LMC and 9 behind the SMC, significantly increasing the number density of known quasars in this region. The

quasars cover the redshift interval $0.2 < z < 2.8$ and apparent mean magnitudes $16.6 \leq \bar{V} \leq 20.1$. Candidate quasars were identified based on aperiodic variability in the MACHO database. MACHO light curves are presented for the newly discovered quasars as well as 12 quasar/AGNs identified in previous studies. The primary contamination during spectroscopic follow-up were quasi- or aperiodic Be/Ae stars in the Magellanic Clouds. Spectroscopic follow-up of quasar candidates in the MACHO database is not yet complete. In the outer LMC, 52 MACHO fields have become accessible for variability-only (§ 2.2) selection since the original candidate selection was run. In addition, ~ 100 candidates have not yet been followed-up from the search presented in this paper. We therefore expect the MACHO database to yield many more sources in the future.

A similar photometric variability selection has been applied to another microlensing database in the Magellanic Clouds, OGLE-II (Eyer 2002), but has not yet been followed-up spectroscopically. We have checked our sample of quasars against the OGLE candidate list presented by Eyer. Four of the MACHO quasars are listed as candidates in this paper, (OGLE candidates: L92, L114, L155, S12), eight OGLE candidates are within $1''$ of spectroscopically confirmed Be stars (L51, L87, L103, L121, L148, L153, S8, S25) and six OGLE candidates are common to our list which have not yet been followed-up spectroscopically. Despite similar quasar candidate selection strategies, the majority of the OGLE candidates did not make our candidate list. This is due in part to our final subjective rejection of Be/Bumper lightcurves: 24 objects classified as quasar candidates by Eyer were considered Be/Bumper star candidates according to MACHO photometry; the remaining objects in the OGLE list either did not pass our minimum variability cut or fell outside MACHO fields. Continued follow-up of both MACHO and OGLE candidates is certain to increase significantly the number quasars in the Magellanic Cloud region.

Quasars behind the Magellanic Clouds are extremely useful tools with which to study the Clouds themselves. Our motivation for this study was to uncover a robust set of reference objects against which to measure the proper motion of the Magellanic Clouds. First epoch *Hubble Space Telescope* images have been scheduled for a subset of quasars presented in this paper; second epoch imaging is expected to allow an estimation of the Cloud's orbital motion with sufficient accuracy to constraint models of the Galactic halo. Quasars are also invaluable tools for a variety of other studies, for example as probes of the Clouds' interstellar medium. We therefore provide finding charts, lightcurves and spectra for all quasars presented in this paper, available electronically at <http://www.ucolick.org/~mgeha/MACHO> or on request from the authors.

We would like to thank Terry Bridges for help with 2dF observations and reductions. This work was performed under the auspices of the U.S. Department of Energy, National Nuclear Security Administration by the University of California, Lawrence Livermore National Laboratory under contract No. W-7405-Eng-48. DM is supported by FONDAP Center for Astrophysics 15010003. MG was supported in part by a grant from IGPP-LLNL UCRP.

REFERENCES

- Alcalde, D. et al. 2002, ApJ, 572, 729
- Alcock, C. et al. 2000, ApJ, 542, 281
- Alcock, C. et al. 1999, PASP, 111, 1539
- Alcock, C. et al. 1997, ApJ, 486, 697
- Anguita, C., Loyola, P., Pedreros, M. H. 2000, AJ, 120, 845
- Bailey, J., Glazebrook, K., & Bridges, T. 2002, 2dF User Manual, Anglo-Australian Observatory
- Blanco, V. M., & Heathcote, S. 1986, PASP, 98, 635
- Cook, K. H. et al. 1995, in Astrophysical Applications of Stellar Pulsation, ASP Conf. Series 83, ed. R. S. Stobies & P. A. Whitelock (San Francisco:ASP), 221
- Crampton, D., Gussie, G., Cowley, A.P., & Schmidtke, P. C., AJ, 114, 2353
- Cristiani, S., Trentini, S., La Franca, F., & Andreani, P. 1997, A&A, 321, 123
- Dobrzycki, A., Groot, P. J., Macri, L. M., & Stanek, K. Z. 2002, ApJ, in press (astro-ph/0202524)
- Dutra, C. M., Bica, E., Claria, J. J., Piatti, A. E., & Ahumada, A. V. 2001, A&A, 371, 895
- Eyer, L. 2002, AcA, submitted (astro-ph/0206074)
- Filipovic, M. D., Haynes, R. F., White, G. L., & Jones, P. A. 1998, A&AS, 130, 421
- Filipovic, M. D., Jones, P. A., White, G. L., Haynes, R. F., Klein, U., & Wielebinski, R. 1997, A&AS, 121, 321
- Gibson, B. K., Giroux, M. L., Penton, S. V., Putman, M. E., Stocke, J. T., Shull, J. M. 2000, AJ, 121,922
- Giveon, U., Maoz, D., Kaspi, S., Netzer, H., & Smith, P. S. 1999, MNRAS, 306, 637
- Haberl, F., Dennerl, K., Filipovic, M. D., Aschenbach, B., Pietsh, W., & Trümper, J. 2001, A&A, 365, L208
- Haberl, F., Pietsch, W. 1999, A&AS, 139, 277
- Hawkins, M. R. S. 2002, MNRAS, 329, 76
- Hewett, P. C., Foltz, C. B., & Chaffee, F. H. 1995, AJ, 109, 1499
- Hjorth, J. et al. 2002, ApJ, 572, L11

- Hook, I. M., McMahon, R. G, Boyle, B. J., & Irwin, M. J. 1994, MNRAS, 268, 305
- Hubert, A. M., & Floquet, M. 1998, A&A, 335, 565
- Jones, B. F., Klemola, A. R., Lin, D. N. C. 1994, AJ, 107, 1333
- Kahabka, P., de Boer, K. S., & Brüns, C. 2001, A&A, 371, 816
- Kahabka, P., Pietsch, W., Filipovic, M. D., & Haberl, F. 1999, A&AS, 136, 81
- Keller, S., Bessell, M. S., Cook, K. H., Geha, M., & Syphers, D. 2002, AJ, accepted (astro-ph/0206444)
- Kroupa, P., Bastian, U. 1997, New Astronomy, 2, 77
- Marx, M., Dickey, J. M., & Mebold, U. 1997, A&AS, 126, 325
- Meusinger, H., & Brunzendorf, J. 2002, A&A, 374, 878
- Prochaska, J. X., Ryan-Weber, E., Staveley-Smith, L. 2002, PASP, accepted (astro-ph/0207479)
- Sasaki, M., Haberl, F., & Pietsch, W. 2000, A&AS, 143, 391
- Schmidtke, P. C., Cowley, A., Crane, J., Taylor, V., McGrath, T., Hutchings, J., & Crampton, D. 1999, AJ, 117, 927
- Sirola, C. J. 1998, ApJ, 495, 659
- Tinney, C. G. 1999, MNRAS, 303, 565
- Welch, D. L., Stetson, P. B. 1993, AJ, 105, 1813

Fig. 1.— *R*-band image of the Large Magellanic Cloud ($8^\circ \times 8^\circ$; G. Bothun 1997, private communication) with the MACHO photometric coverage indicated by large numbered squares. North is up, East is to the left in this image. Small black and white symbols indicate quasars discussed in this paper. The distribution of quasars is biased due to early unavailability of analyzed MACHO fields and incomplete spectroscopic follow-up coverage.

Fig. 2.— *R*-band image of the Small Magellanic Cloud ($3^\circ \times 5^\circ$) with the MACHO photometric coverage indicated. Small black and white symbols indicate presented quasars.

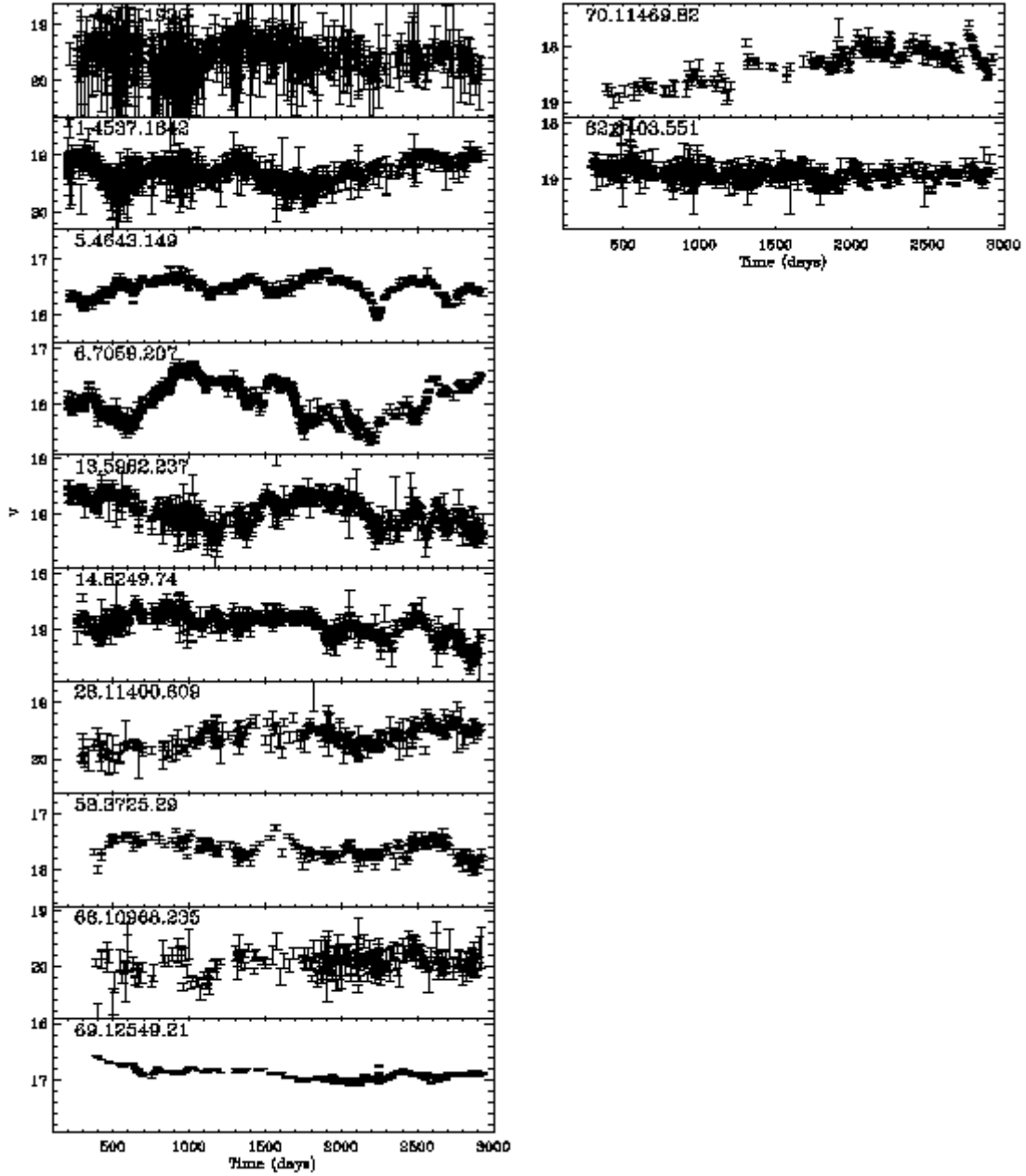


Fig. 3.— V -band MACHO lightcurves for 12 quasar/AGNs in the MACHO database previously known behind the LMC. See Table 1 for reference to the discovery paper of each source.

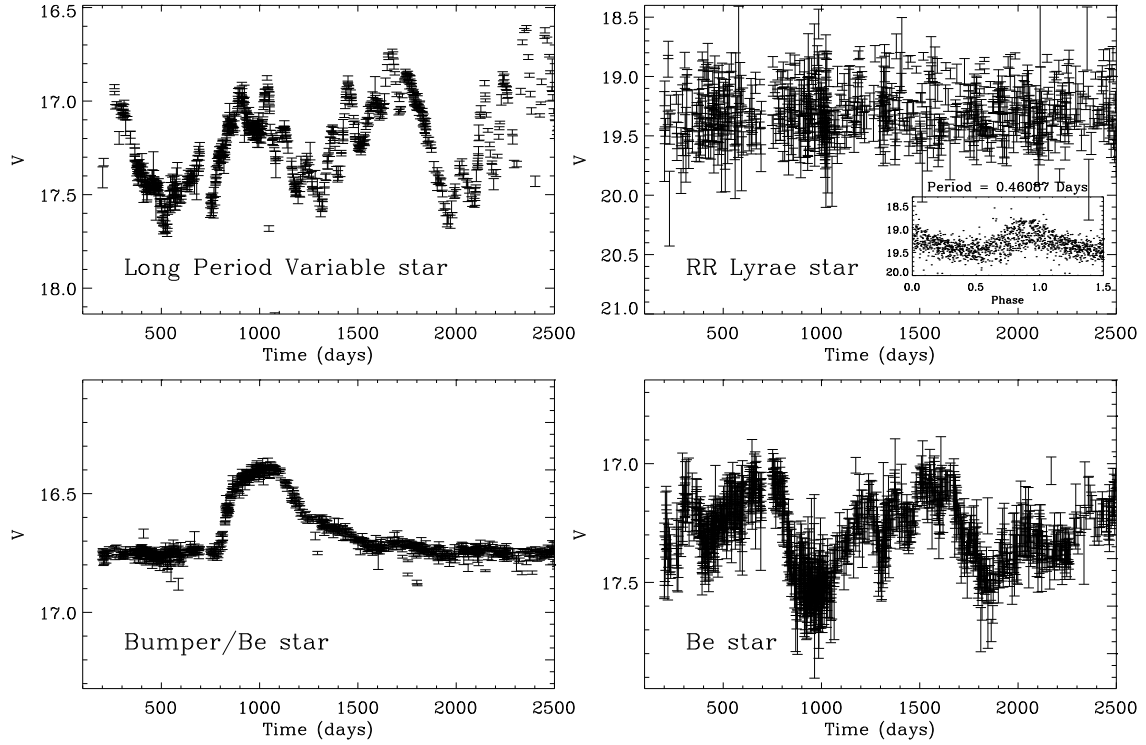


Fig. 4.— V -band lightcurves of variable stars in the MACHO database. Examples of stars rejected by our quasar selection technique are (*top, left panel*) red, long period variable stars, (*top, right panel*) RR Lyrae stars, in this example phased with a 0.46 day period (panel inset), and (*bottom, left panel*) blue variable ('Bumper') stars. The main contaminant to our quasar candidate search were emission line Be stars with quasi- to aperiodic lightcurves (*bottom, right panel*).

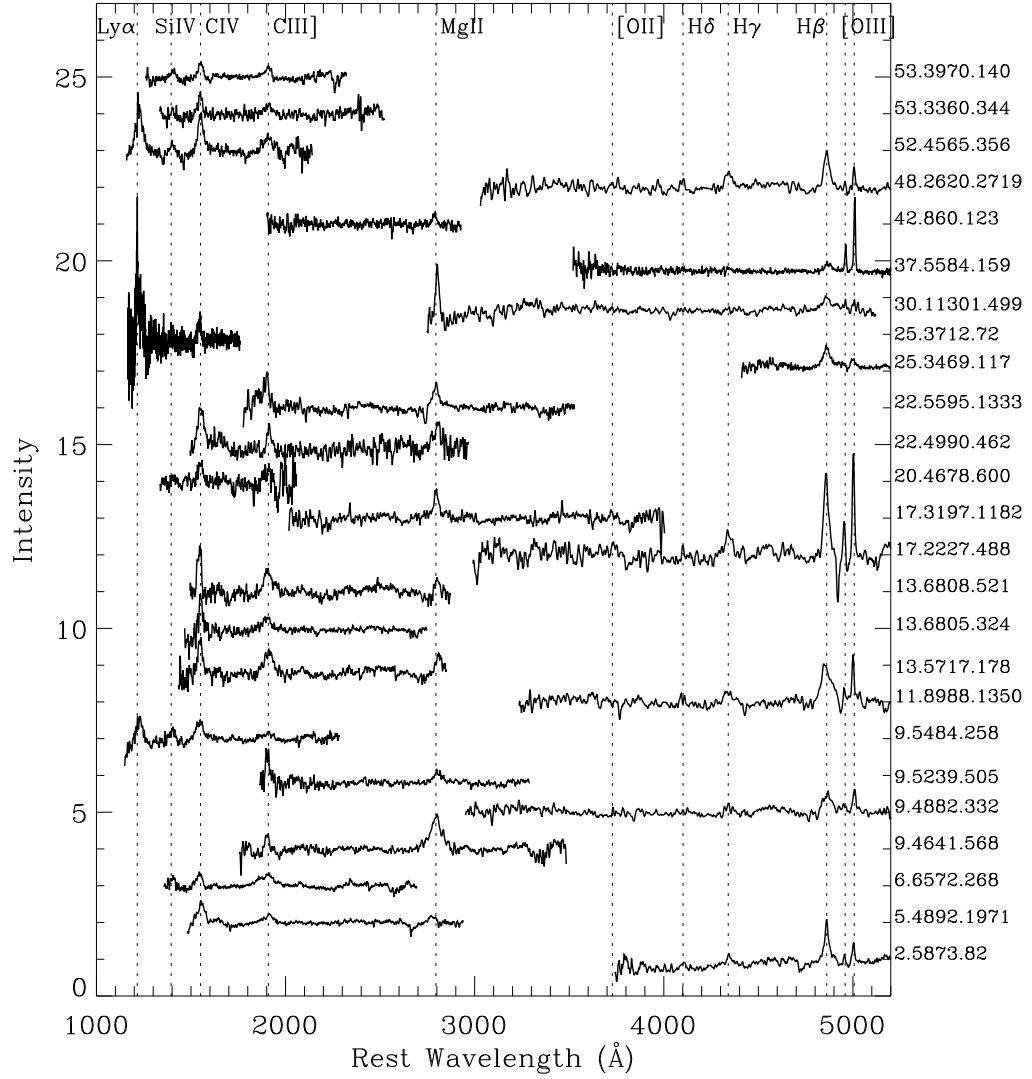


Fig. 5.— Low resolution spectra, corrected to the rest frame, for the 47 MACHO quasars presented. Source names appear to the right of each spectrum. The spectra have been normalized, smoothed and arbitrarily shifted in intensity for display purposes.

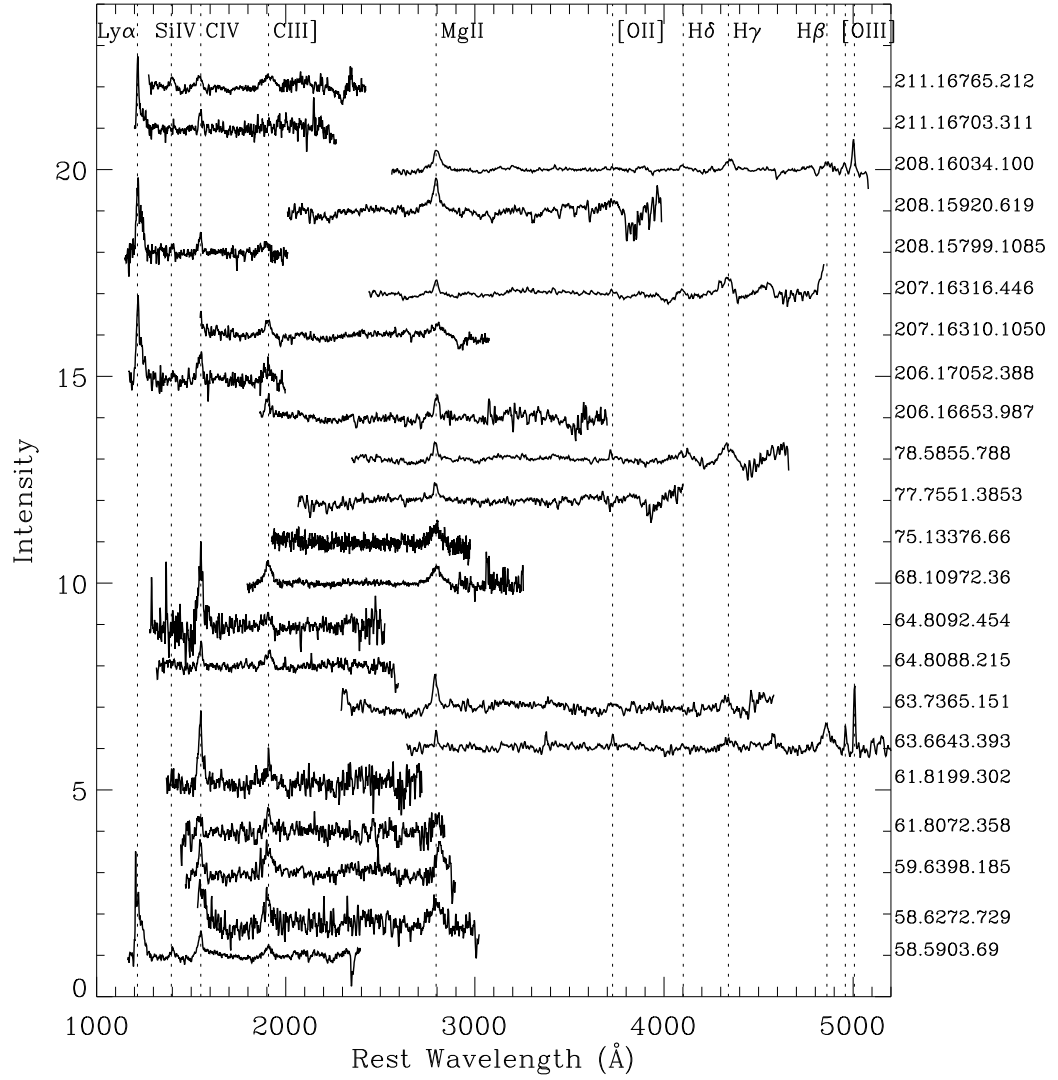


Fig. 5.— continued.

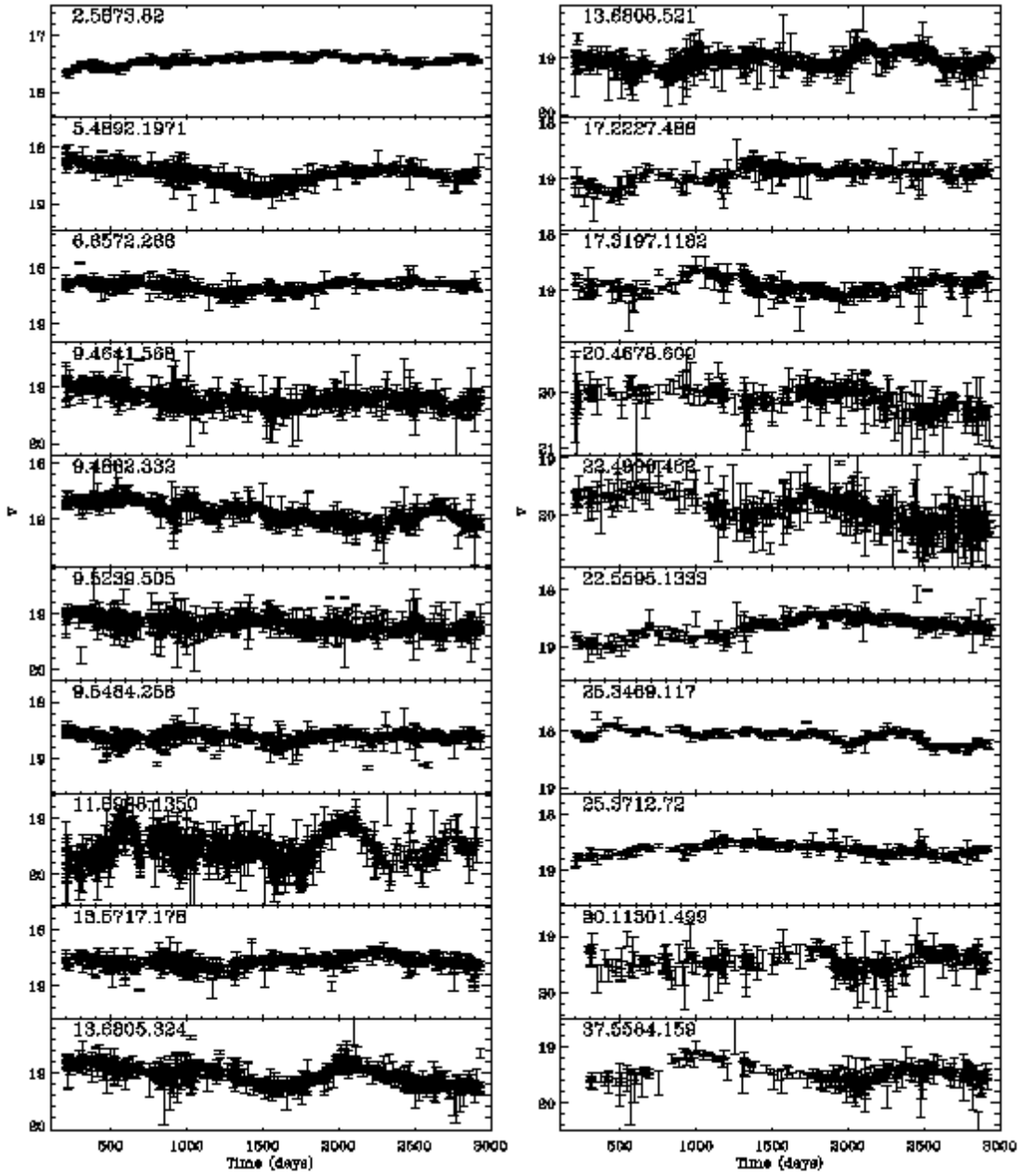


Fig. 6.— *V*-band MACHO lightcurves for quasars behind the LMC presented in this paper. The *y*-axis scale is the same for all objects, spanning 2.0 magnitudes centered on the weighted mean *V*-band brightness of each source. The lightcurves cover 7.5 years; the zero point of the times axis corresponds to JD 2448623.5, or UT 1992 January 2.0.

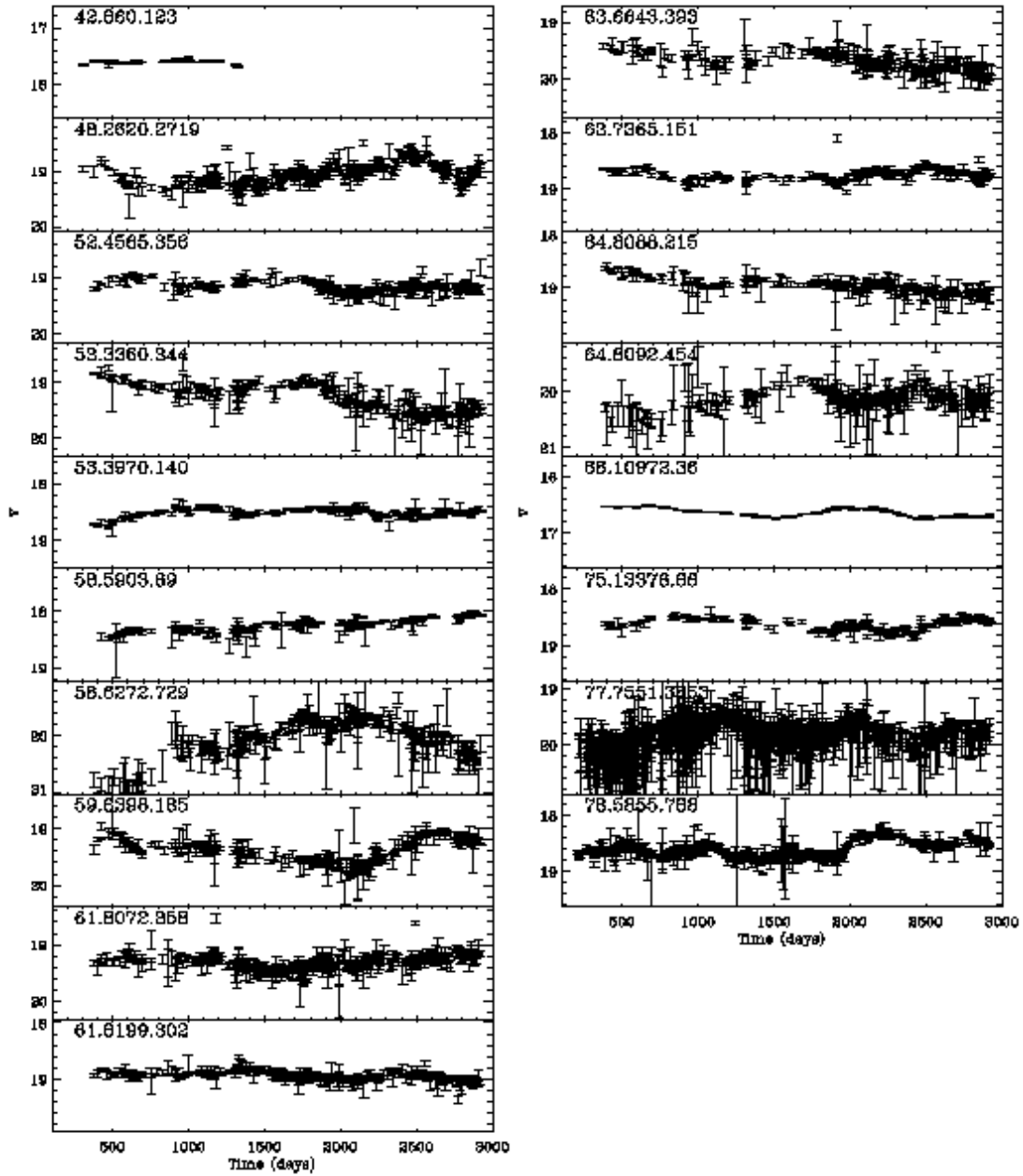


Fig. 6.— continued.

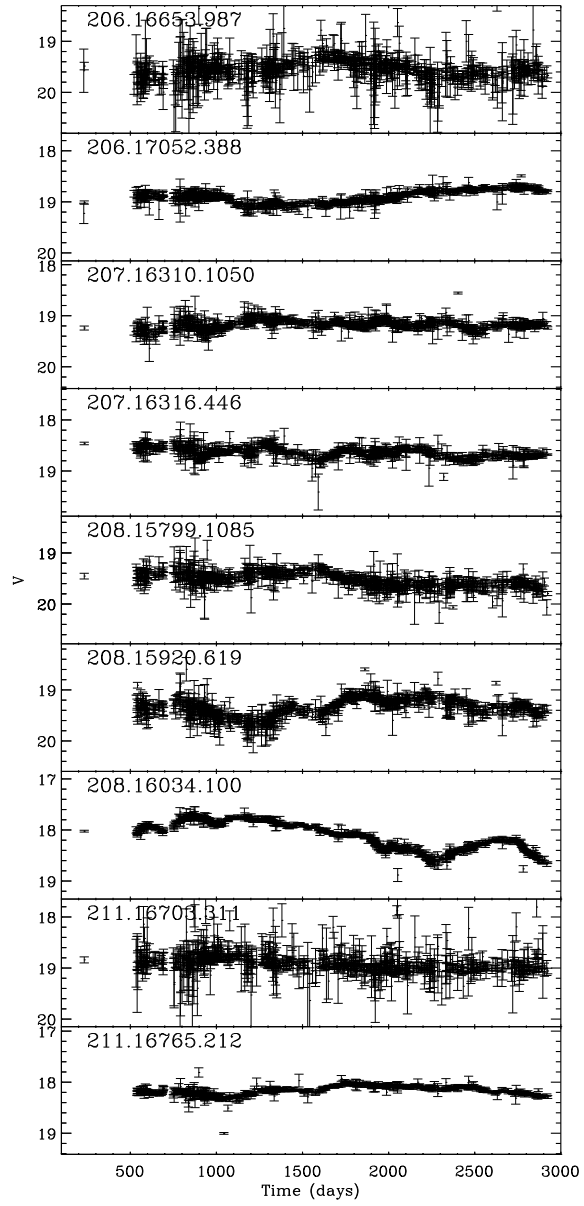


Fig. 7.— V-band MACHO lightcurves for 9 quasars discovered behind the SMC. See the caption for Figure 6.

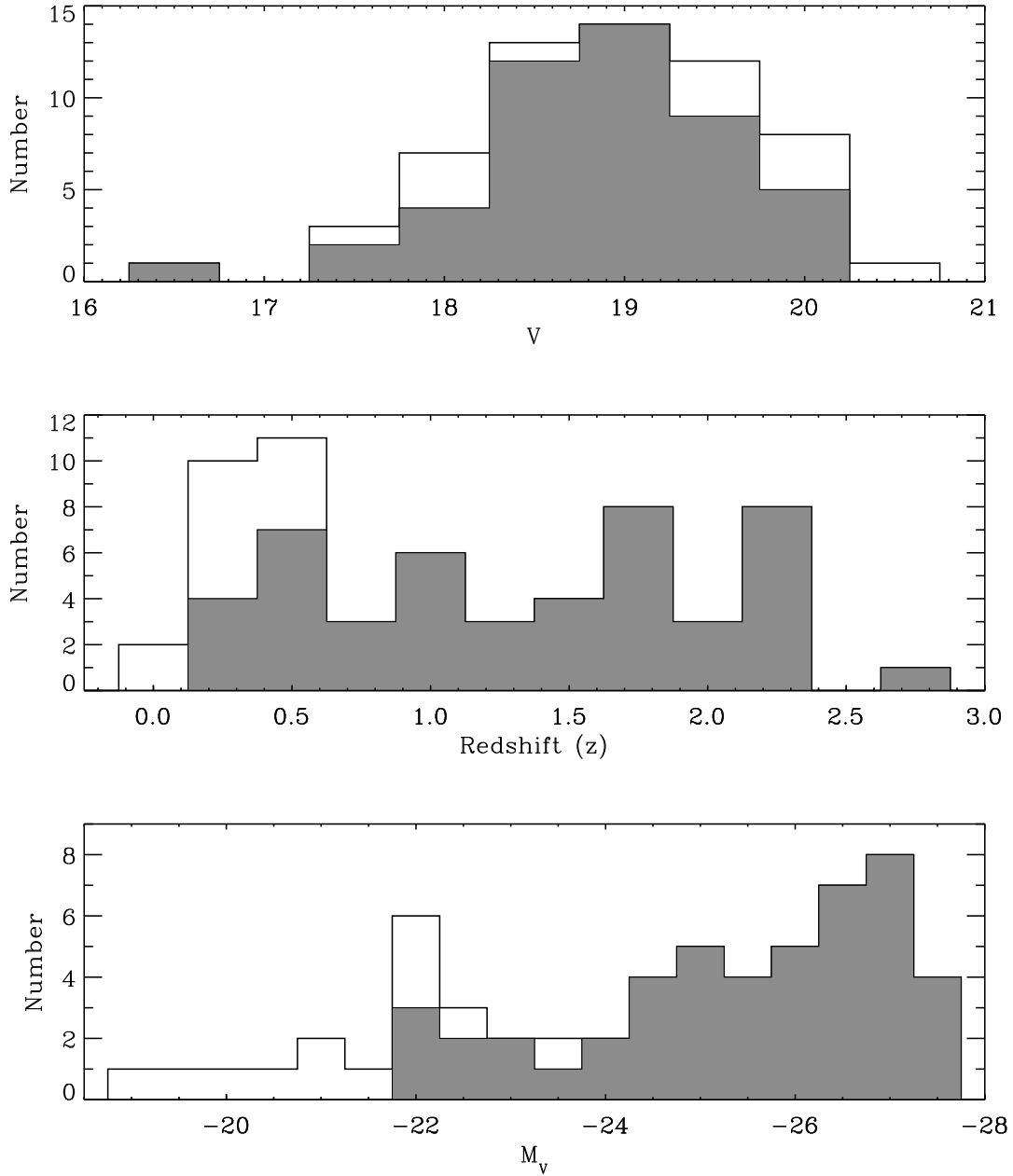


Fig. 8.— Histograms of MACHO quasars as a function (*from top to bottom*) of mean apparent V -band magnitude, redshift, z , and absolute magnitude, M_V . The shaded region of each histogram represents quasars identified in this study behind the Magellanic Clouds.

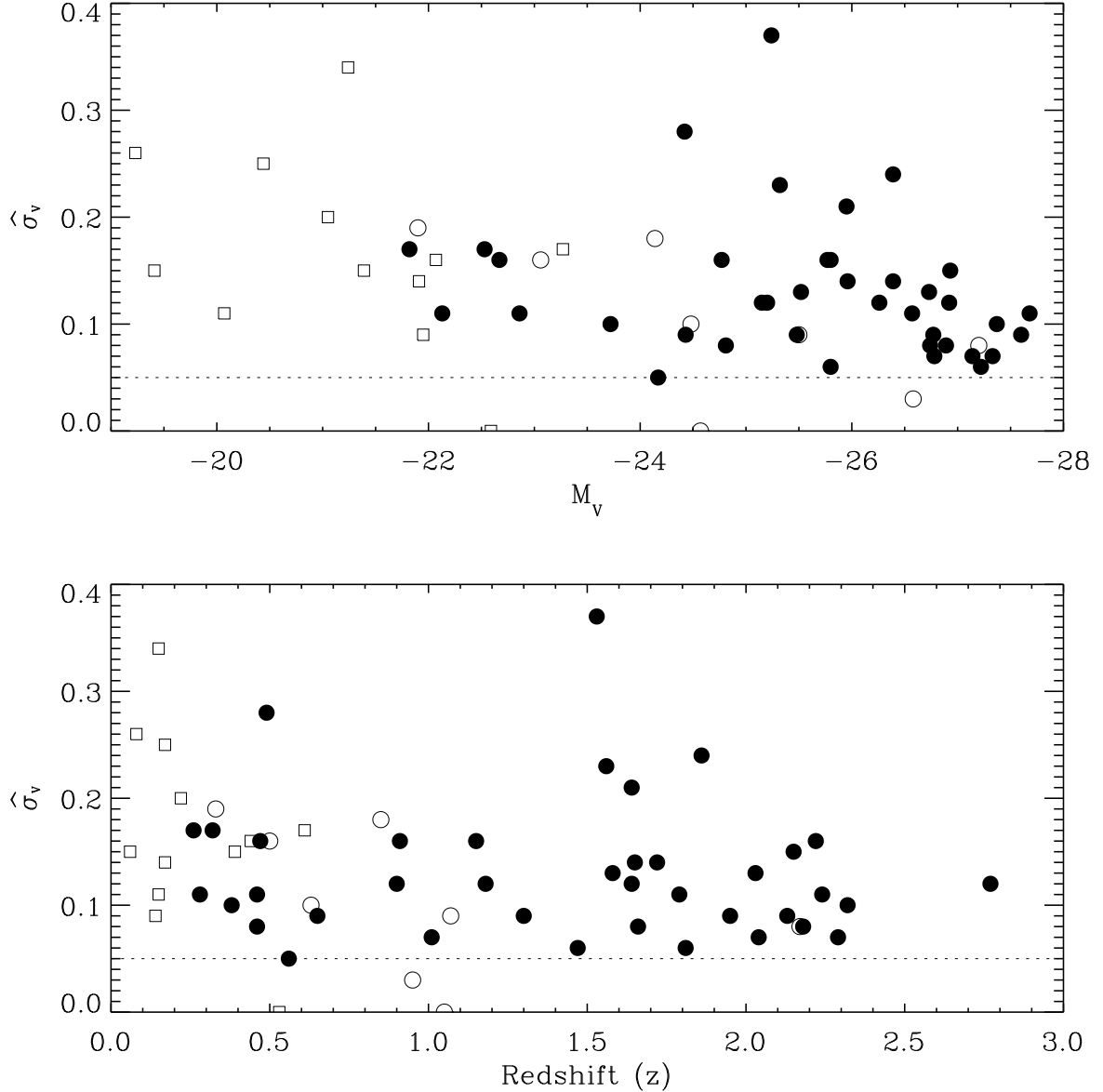


Fig. 9.— The intrinsic photometric variability $\widehat{\sigma}_V$ as a function of absolute magnitude, M_V (*top panel*) and redshift (*bottom panel*). The dotted line indicates the variability selection requirement of $\widehat{\sigma}_V \geq 0.05$. Solid circles represent MACHO quasars discovered via variability-only selection, open circles indicate quasars discovered as variable counterparts to X-ray and radio sources for which the amount of variability required for selection was relaxed. Open squares represent previously discovered quasar/AGNs.

Table 1. Previously Identified AGN in the MACHO Database

Source Name	MACHO ID	α (J2000)	δ (J2000)	\bar{V}	$(\bar{V}-\bar{R})$	z	M_V	n_V	Ref
050736.52-684751.7	1.4418.1930	05:07:36.39	-68:47:52.94	20.05	0.14	0.53	-22.59	1071	1
050833.29-685427.5	1.4537.1642	05:08:31.89	-68:55:10.66	19.75	0.16	0.61	-23.27	1137	1
RX J0509.2-6954	5.4643.149	05:09:15.49	-69:54:16.75	17.95	0.28	0.17	-21.91	939	2
RX J0524.0-7011	6.7059.207	05:24:02.31	-70:11:08.95	18.26	0.42	0.15	-21.24	980	2
RX J0517.4-7044	13.5962.237	05:17:17.03	-70:44:02.46	19.33	0.40	0.17	-20.44	894	2
RX J0531.5-7130	14.8249.74	05:31:31.60	-71:29:47.78	19.36	0.23	0.22	-21.05	869	2
RX J0550.5-7110	28.11400.609	05:50:31.22	-71:09:58.47	20.08	0.26	0.44	-22.07	322	2
RX J0503.1-6634	53.3725.29	05:03:04.04	-66:33:46.62	18.10	0.41	0.06	-19.41	268	2
RX J0547.8-6745	68.10968.235	05:47:45.13	-67:45:5.745	20.45	0.51	0.39	-21.39	263	2
[HB89]0557-672	69.12549.21	05:57:22.41	-67:13:22.16	17.41	0.38	0.14	-21.95	254	3
RX J0550.6-6637	70.11469.82	05:50:33.31	-66:36:52.96	18.19	0.65	0.08	-19.23	248	2
RX J0532-6920	82.8403.551	05:31:59.66	-69:19:51.12	19.40	0.31	0.15	-20.07	851	2

Note. — Weighted average magnitudes \bar{V} and colors $(\bar{V}-\bar{R})$ determined from MACHO photometry; n_V is the number of MACHO photometric data points over the 7.5-year monitoring period. Redshifts, z , are taken from discovery papers as follows: 1 = Dobrzycki et al. (2002), 2 = Schmidtke et al. (1999), 3 = Blanco & Heathcote (1986).

Table 2. MACHO Quasars Behind the Large Magellanic Cloud

MACHO ID	α (J2000)	δ (J2000)	\bar{V}	$\overline{(V-R)}$	z	M_V	n_V	Notes
2.5873.82	05:16:28.78	-68:37:02.38	17.44	0.44	0.46	-24.81	967	
5.4892.1971	05:10:32.32	-69:27:16.90	18.45	0.33	1.58	-26.73	960	
6.6572.268	05:20:56.93	-70:24:52.50	18.33	0.24	1.81	-27.22	989	
9.4641.568	05:08:45.95	-70:05:00.92	19.20	0.30	1.18	-25.20	993	
9.4882.332	05:10:23.18	-70:07:36.12	18.83	0.32	0.32	-22.53	1004	
9.5239.505	05:12:59.56	-70:30:24.76	19.18	0.36	1.30	-25.48	992	
9.5484.258	05:14:12.05	-70:20:25.64	18.61	0.33	2.32	-27.37	997	
11.8988.1350	05:36:00.50	-70:41:28.86	19.52	0.30	0.33	-21.90	1008	a
13.5717.178	05:15:36.02	-70:54:01.65	18.56	0.37	1.66	-26.74	921	
13.6805.324	05:22:47.23	-71:01:31.08	18.66	0.35	1.72	-26.39	959	
13.6808.521	05:22:47.69	-70:47:34.82	19.02	0.32	1.64	-26.26	942	
17.2227.488	04:53:56.55	-69:40:35.96	18.88	0.32	0.28	-22.13	449	
17.3197.1182	05:00:17.56	-69:32:16.32	18.88	0.32	0.90	-25.15	435	
20.4678.600	05:08:54.08	-67:37:35.57	20.06	0.24	2.22	-25.80	372	
22.4990.462	05:11:40.77	-71:00:32.95	19.82	0.38	1.56	-25.32	580	
22.5595.1333	05:15:22.94	-70:58:06.77	18.55	0.29	1.15	-25.77	572	
25.3469.117	05:01:46.68	-67:32:41.81	18.07	0.26	0.38	-23.72	376	
25.3712.72	05:02:53.65	-67:25:46.44	18.61	0.31	2.17	-27.20	372	b
30.11301.499	05:49:41.63	-69:44:15.86	19.41	0.35	0.46	-22.86	309	
37.5584.159	05:15:04.72	-71:43:38.62	19.43	0.66	0.50	-23.06	275	c
42.860.123	04:46:11.14	-72:05:09.80	17.60	0.29	0.95	-26.58	50	d
48.2620.2719	04:56:14.19	-67:39:10.81	19.03	0.32	0.26	-21.82	368	
52.4565.356	05:08:30.64	-67:02:30.05	19.16	0.21	2.29	-26.78	257	
53.3360.344	05:00:54.00	-66:44:01.34	19.22	0.22	1.86	-26.39	268	
53.3970.140	05:04:36.01	-66:24:17.03	18.50	0.27	2.04	-27.14	272	
58.5903.69	05:16:36.76	-66:34:36.92	18.20	0.26	2.24	-27.68	251	
58.6272.729	05:18:51.97	-66:09:56.70	19.85	0.35	1.53	-25.24	342	
59.6398.185	05:19:28.02	-65:49:50.50	19.33	0.36	1.64	-25.95	284	
61.8072.358	05:30:07.93	-67:10:27.20	19.33	0.27	1.65	-25.96	388	
61.8199.302	05:30:26.81	-66:48:55.31	18.94	0.25	1.79	-26.57	392	
63.6643.393	05:20:56.45	-65:39:04.79	19.65	0.41	0.47	-22.67	250	
63.7365.151	05:25:14.29	-65:54:45.93	18.72	0.33	0.65	-24.43	252	
64.8088.215	05:30:09.06	-66:07:01.05	18.96	0.23	1.95	-26.77	257	
64.8092.454	05:30:08.75	-65:51:24.27	20.10	0.20	2.03	-25.52	258	
68.10972.36	05:47:50.18	-67:28:02.44	16.63	0.28	1.01	-27.33	267	
75.13376.66	06:02:34.25	-68:30:41.51	18.63	0.26	1.07	-25.50	241	e
77.7551.3853	05:27:16.19	-69:39:33.96	19.75	0.21	0.85	-24.14	1471	f
78.5855.788	05:16:26.23	-69:48:19.39	18.61	0.22	0.63	-24.48	878	g

Note. — Weighted average magnitudes \bar{V} and colors $\overline{(V-R)}$ determined from MACHO photometry; n_V is the number of MACHO photometric data points. Redshifts, z , determined from spectra discussed in §3. The majority of quasars were selected as candidates based on photometric variability alone. Variable counterparts to X-ray and radio sources are indicated in the table notes as follows: (a) RX J0536.0-7041, (b) 1WGA J0508.9-6737 (c) [HP99] 1306, (d) PMN J0446-7205, (e) PMN J0603-6830, (f) 1WGA J0527.2-6939, (g) [HP99] 1019.

Table 3. MACHO Quasars Behind the Small Magellanic Cloud

MACHO ID	α (J2000)	δ (J2000)	\bar{V}	$(\overline{V-R})$	z	M_V	n_V	Notes
206.16653.987	01:01:27.81	-72:46:14.37	19.51	0.25	1.05	-24.57	794	
206.17052.388	01:07:21.71	-72:48:45.76	18.85	0.23	2.15	-26.93	810	
207.16310.1050	00:55:59.61	-72:52:45.15	19.17	0.31	1.47	-25.80	850	
207.16316.446	00:55:34.70	-72:28:34.23	18.64	0.19	0.56	-24.17	822	a
208.15799.1085	00:47:15.76	-72:41:12.24	19.52	0.26	2.77	-26.92	861	
208.15920.619	00:49:34.43	-72:13:08.99	19.28	0.18	0.91	-24.77	858	
208.16034.100	00:51:16.89	-72:16:51.06	18.03	0.25	0.49	-24.42	878	
211.16703.311	01:02:14.36	-73:16:26.80	18.92	0.34	2.18	-26.89	791	
211.16765.212	01:02:34.73	-72:54:22.20	18.15	0.29	2.13	-27.60	795	

Note. — See notes for Table 2. Candidate identified as variable counterpart to X-ray source: (a) RX J0055.6-7228